OPEN ACCESS

IOP Publishing | Vietnam Academy of Science and Technology

Advances in Natural Sciences: Nanoscience and Nanotechnology

Adv. Nat. Sci.: Nanosci. Nanotechnol. **6** (2015) 013002 (8pp)

doi:10.1088/2043-6262/6/1/013002

Review

Hydrogen storage in Ti, V and their oxides-based thin films*

Z Tarnawski[1], K Zakrzewska[2], N-T H Kim-Ngan[3], M Krupska[3], S Sowa[3], K Drogowska[1], L Havela[4] and A G Balogh[5]

[1] Faculty of Physics and Applied Computer Science, AGH University of Science and Technology, 30-059 Kraków, Poland

[2] Faculty of Computer Science, Electronics and Telecommunication, AGH University of Science and Technology, 30-059 Kraków, Poland

[3] Institute of Physics, Pedagogical University, 30-084 Kraków, Poland

[4] Faculty of Mathematics and Physics, Charles University, Ke Karlovu 5, 12116 Prague, Czech Republic

[5] Institute of Materials Science, Technische Universität Darmstadt, 64287 Darmstadt, Germany

E-mail: tarnawsk@agh.edu.pl

Received 9 November 2014

Accepted for publication 20 November 2014

Published 16 December 2014

Abstract

We have investigated the hydrogen storage ability and the effect of hydrogenation on structure and physical properties of Ti/V and their oxides-based thin films. A series of Ti–TiO_2 and VO_x–TiO_2 thin films with different layer structures, geometries and thicknesses have been prepared by the sputtering technique on different (Si(111), SiO_2, C) substrates. For the Ti–TiO_2–Ti films up to 50 at.% of hydrogen can be stored in the Ti layers, while the hydrogen can penetrate without accumulation through the TiO_2 layer. A large hydrogen storage was also found in some V_2O_5–TiO_2 films. Hydrogen could also remove the preferential orientation in the Ti films and induce a transition of V_2O_5 to VO_2 in the films.

Keywords: titan oxides, vanadium oxides, multilayers, crystal structure, hydrogen storage

Mathematics Subject Classification: 2.00, 5.00, 5.13

1. Introduction

Hydrogen has been generally accepted as a fuel in the future. There is currently a lot of hope in hydrogen-based energy. The construction of hydrogen-based energy systems brings up new issues, such as the interaction of hydrogen and matter in the solid state, the search for hydrogen storage materials etc This work is a review of our recent work of investigations of the hydrogen storage as well as the effect of hydrogenation on structure and physical properties of Ti and TiO_2-based thin films. Some new data obtained for V and VO_x-based thin films will be also presented.

Titanium dioxide, TiO_2, has been widely used as pigments and paints [1], in the optical coatings for laser mirrors, interference filters, etc [2, 3]. Its photocatalytic properties (i.e. breaking water into hydrogen and oxygen on TiO_2 electrodes) have been discovered by Fujishima and Honda since 1972 [4]. TiO_2 nowadays finds various novel applications in photoelectrochemistry, photocatalysis, solar cells and gas sensors [5–7]. For an extensive overview of the development of TiO_2-based photocatalysis and its future prospects, see [8–10].

An increased interest in TiO_2 has been recently focused on the development of its nanostructured forms (nanotubes, nanorods, etc) for renewable energy sources and hydrogen economy. For example, TiO_2 nanotubes grown on Ti substrates by anodization could be used for hydrogen storage [11]. Metal–insulator–metal (MIM) structures such as Ti/TiO_2/Pt were proposed for resistance random access

* Invited talk at the 7th International Workshop on Advanced Materials Science and Nanotechnology IWAMSN2014, 2-6 November, 2014, Ha Long, Vietnam.

memories (ReRAM) [12, 13]. Light induced metal-semiconductor reversible transition at room temperature has been demonstrated for TiO_x nanoparticles making it a promising material for high density storage media [14].

The vanadium oxide family (V_2O_5, V_2O_3, VO_2) is among the most attractive class of smart materials exhibiting semiconductor–metal transition. Vanadium pent-oxide (V_2O_5), the most stable vanadium oxide having a wide band gap and being an n-type semiconductor material, has been used especially as optical and electrical devices, e.g. V_2O_5 thin films can be applied in electrochromic and electrochemical devices [15] and microscale batteries [16]. A large interest is focusing on investigations of TiO_2–V_2O_5 thin films to gain the optimal electrochromic properties [17] regarding their potential applications for electrochromic smart windows. The interaction of V_2O_5 with TiO_2 would strongly affect the structural properties and reactivity of V_2O_5; in particular, it leads to V_2O_5 dispersion [18, 19]. We notice here that due to oxygen reduction by using e.g. hydrogen, V_2O_5 can be converted to vanadium dioxide VO_2 and a complex mixture such as V_4O_7 and V_5O_9 before V_2O_3 is reached. The promoting effect of a titanium oxide support on the catalytic properties of vanadium oxide is widely recognized [20]. Investigations of thermochromic properties have revealed that VO_2–TiO_2 multilayers have a higher luminous transmittance than that of single VO_2 film and could yield a large change of solar transmittance at both temperatures below and above semiconductor–metal transition temperature (~333 K) of VO_2 [21].

Introduction of hydrogen into the crystal lattice in general leads to a modification of both crystal and electronic structure. Hydrogen absorption brings a relatively small perturbation to the system (e.g. the lattice expansion and the hydrogen bonding with other atoms in the lattice). It, however, often implies some new and interesting features in the systems. Thin films and multilayers often play an important role in the improvement of hydrogen absorption rate as well as the chemical and crystal structure stability. On the other hand, the atom mixing, diffusion across the interfaces and precipitation of nanoparticles may also affect the hydrogen uptake-release cycling as well as the thermodynamic properties of the films.

We aim at characterization of the film structure and properties of the TiO_2-based thin films, in particular the interlayer properties and the influence of hydrogen intake on the microstructure and electronic structure of the films. Numerous TiO_2-based thin films, consisting of TiO_2, Ti and VO_x layers with a different layer structure (e.g. with single-, bi- and tri-layer structure of different layer sequences), have been prepared by means of sputtering technique and investigated. Selected films subjected for hydrogenation were then investigated focusing on film stability, hydrogen uptake and hydrogen storage under different conditions. Details of the experiments and the main outcome of our study are presented in the next sections.

2. Experimentals

Thin films consisted of Ti, TiO_2 and VO_x layers with different layer sequences and different layer-thicknesses have been deposited by means of magnetron dc pulse sputtering system [22] on Si(111), silica SiO_2 and C-foil substrates. Our analysis of all investigated layers indicates the presence of TiO_2 rutile, while several vanadium oxide forms (V_2O_5, VO_2…) can exist. For the selected film, an additional Pd layer was deposited on the film surface by MBE technique.

Selected films with chosen film-structure have been subjected to hydrogenation at atmospheric atmosphere (1 bar) and at 300 °C (so-called hydrogen charging) and/or at high hydrogen pressure up to 102 bar and at room temperature (RT) with different times. For the VO_x–TiO_2 series, some samples were charged with hydrogen at 1 bar only once, while some were charged twice. Each charging was for 3 h.

For investigating the possibility of enhancement of hydrogen absorption in the thin film system, an additional palladium layer was deposited on a chosen film by molecular beam epitaxy (MBE) technique.

The film chemical composition, depth profile, layer thickness and structure were determined by combined analysis of x-ray diffraction (XRD), x-ray reflectometry (XRR), Rutherford back-scattering (RBS) and optical spectrophotometry. In order to compare the layer-thickness determination from three independent complementary methods, we also evaluated the layer thickness in nm from RBS data. More details of RBS analysis are described elsewhere [23, 24].

The hydrogen profile was determined by means of a secondary ion mass spectroscopy (SIMS) and N-15 Nuclear Reaction Analysis (^{15}N-NRA method). SIMS was carried out by using Cs^+ primary ions recording positive secondary ions by a CAMECA ims 5f equipment. The reaction $^{15}N + {}^1H \rightarrow {}^{12}C + \alpha + \gamma$ (4.965 MeV) at a resonance energy of 6.417 MeV was used for the ^{15}N-NRA method to obtain the results. For data evaluation the computer code SRIM was used.

3. Results and discussion

3.1. Hydrogen storage in Ti–TiO_2 films

Hydrogen storage in these systems have been thoroughly investigated and reported in our previous publications [25–27]. Our investigations revealed that:

I. On the as-deposited films of Ti-TiO_2 system:
   1. Single Ti nucleates and grows as a compact layer on the well-defined (111) plane of Si wafer– Ti/Si(111). Interdiffusion was not found at the Ti/Si interface, i.e. a sharp interface was always obtained. This Ti film exhibits a strong preferred orientation with (00.1) plane parallel to the substrate,
   2. A small amount of interdiffusion was found at the Ti–TiO_2 interface of the bi-layer film and at both Ti–TiO_2 and TiO_2–Ti interfaces of the tri-layer film. The intermediate TiO_2 layer exhibits columnar structure

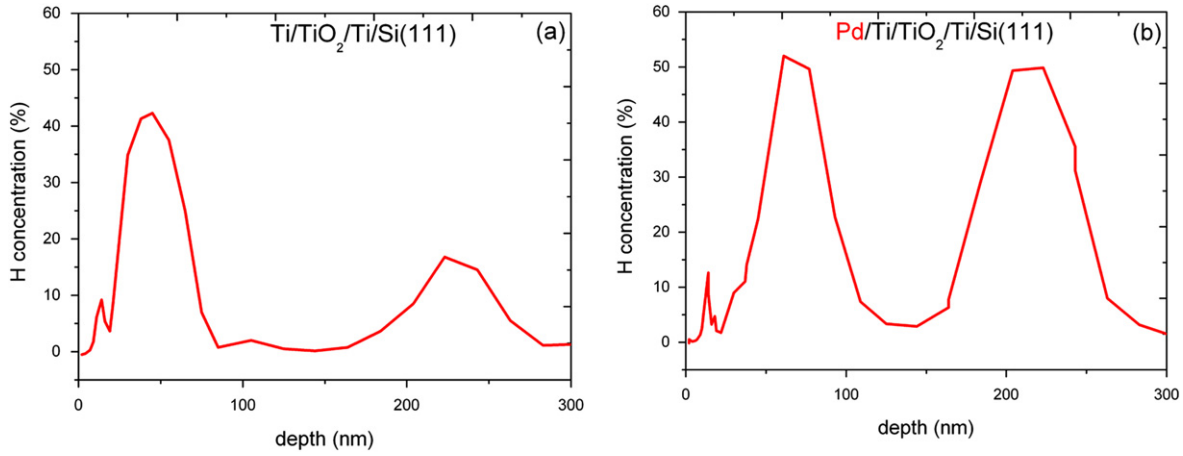

Figure 1. Comparison of the hydrogen profile determined by ^{15}N-NRA for the Ti/TiO_2/Ti/Si(111) film (a) without covering Pd and with Pd cover (b). The hydrogen charging was at 1 bar and at 300 °C.

and there is some intergrowth between the Ti and TiO_2 layers. The interdiffusion is attributed to Ti diffusion along the channels formed between the TiO_2 columns,

3. More precise determination of layer thickness and element concentration, in particular the oxygen concentration, can be obtained for films deposited on C-foils. However, in this case a strong carbon diffusion (up to 10 at.%) into the film was observed. If the film is thin (the layer thickness <30 nm), the carbon can be found even in the surface layer due to carbon segregation from the substrates,

II. On hydrogen-charged Ti–TiO_2 films:

4. High hydrogen concentration (storage), up to a value of over 40–50 at.%, was obtained for the top Ti-layer,
5. Palladium could act as a good catalyst for hydrogen diffusion in the Ti–TiO2–Ti films. Without covering the film surface by palladium, the hydrogen concentration in the bottom Ti layer has reached only 15 at.%, whereas it increases up to 40 at.% when the film was covered by palladium,
6. Hydrogen could be moved through TiO2 layer without any accumulation there,
7. The preferential orientation in the Ti films was destroyed/disappeared by hydrogen charging under high pressures (pH2 = 100 bar),
8. Large swelling effect was observed for the thick Ti layer (>240 nm) after hydrogen charging at 100 bar. The enhanced hydrogen concentration (enhanced storage) leads to an increase of the film thickness up to 150% of its original value.

The hydrogen profile determined by ^{15}N-NRA for the Ti/TiO_2/Ti/Si(111) films revealing the large hydrogen storage up to 40–50 at.% is shown in figure 1. More detailed results can be found in our previous publication [26].

3.2. Hydrogen storage in VO_x–TiO_2 films

Prior to the hydrogenation experiments, we have studied thoroughly the properties of layered structures of numerous VO_x–TiO_2 films with different film-geometry and thickness. The measured and simulated RBS spectra for the 5 films deposited on silica SiO_2 substrates are shown in figure 2. Estimated layer composition and thickness for each layer in the films are given in table 1.

The RBS spectrum of V_2O_5/SiO_2 film (VS1) is characterized by a large V-peak at energy around 1250 keV from the film, a steep Si- and O edge from the substrate, respectively, at 960 keV and 616 keV. Oxygen is present both in the film and in the substrate, thus no separated oxygen signal from the film was observed; its presence implies some increase of the signal on the left-hand side of the O-edge (below 616 keV) in the RBS spectra. The film structure can be described as follows: 1) the upmost surface layer of the film indeed consists of the most stable and common vanadium oxide V_2O_5 with a thickness of 13 nm (denoted as layer 1 of sample VS1 in table 1), 2) beneath the V_2O_5 layer is a thick layer with a composition of V_2O_{5-x} (layer 2) with x increasing from 0 to 3.0 and thickness of 51 nm, 3) beneath the V_2O_{5-x} layer is the stoichiometric VO_2 layer with a thickness of 15 nm (layer 3) and 4) an interface layer consisted of a mixture of $VO_2 + SiO_2$ was formed as a consequence of V diffusion deeply into the SiO_2 substrate (revealed by the non-zero background between the V-peak and Si-edge). A more detail analysis of the mixture layer V_2O_{5-x} (layer 2, thickness 51 nm) indicates that it consists of two sub-layers, the first one with a thickness of 24 nm beneath the surface V_2O_5 layer 1) is as a mixture of V_2O_5, V_2O_7 (i.e. $x = 1.5$) and V_5O_9 ($x = 1.4$), while the second one (above the VO_2 layer 3) with a thickness of 27 nm is a mixture of V_2O_3 layer ($x = 2.0$) and VO ($x = 3.0$).

Our results indicate that during film deposition, first the VO_2 layer was formed on SiO_2 substrate (with an oxygen content of 33.3%). With increasing deposition time, the

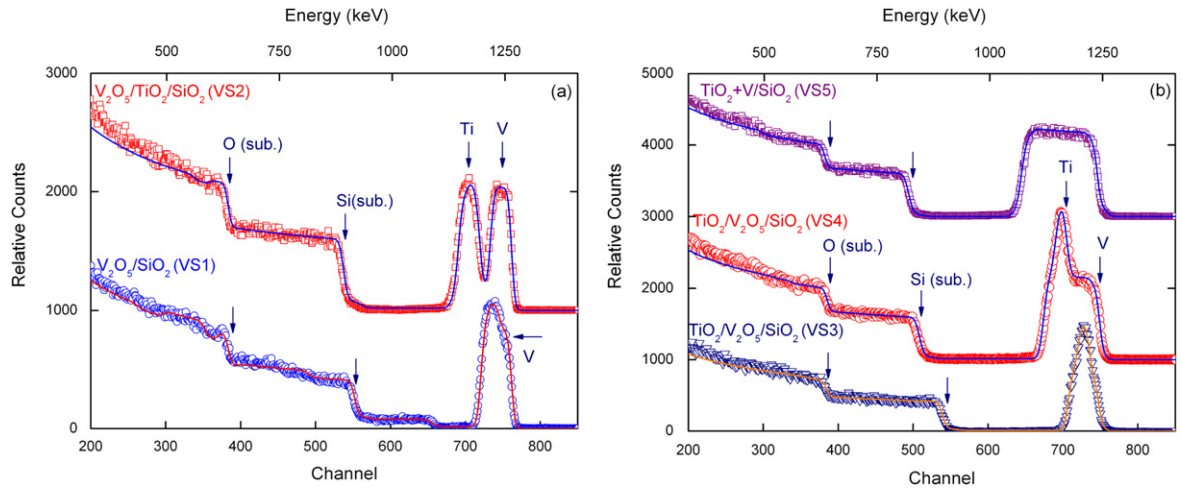

Figure 2. Random RBS (markers) and SIMNRA (lines) simulated spectra for (a) 79 nm thick V_2O_5/SiO_2 (sample VS1) and 122 nm thick $V_2O_5/TiO_2/SiO_2$ (VS2) and (b) 117 nm thick $TiO_2/V_2O_5/SiO_2$ (VS3), 184 nm thick $TiO_2/V_2O_5/SiO_2$ (VS4) and 193 nm thick $TiO_2 + V/SiO_2$ (VS5) after deposition. RBS experiments were performed with the incident He^+ ion energy of 1.7 MeV and the backscattering angle of 171°. The films are denoted by nominal chemical composition and the estimated total thickness (see table 1). The curves were normalized and shifted for clarity.

Table 1. Chemical composition of TiO_2–VO_x films deposited on silica SiO_2 substrates after deposition (as-deposited films): V_2O_5/SiO_2 (denoted as sample VS1), $V_2O_5/TiO_2/SiO_2$ (VS2), $TiO_2/V_2O_5/SiO_2$ (VS3 and VS4, with the same layer geometry but different thickness) and $TiO_2 + V/SiO_2$ (VS5). The layer-thickness of each layer (d (nm)), the percentage (%) of each type of oxides (TiO_2, V_2O_5, VO_2) presented in the film are estimated using SIMNRA and the mass density of the bulk (see text). Layer (1) denotes the surface layer. The layer (2) of sample S1 consists of V_2O_{5-x} with $x = 0$–3.0 (see text).

	Layer	V_2O_5 (%)	TiO_2 (%)	VO_2 (%)	SiO_2 (%)	d (nm)	D (nm)
V_2O_5/SiO_2	1	100	—	—	—	13	79
(VS1)	2	100 (V_2O_{5-x})	—	—	—	51	—
—	3	—	—	100	—	15	—
$V_2O_5/TiO_2/SiO_2$	1	100	—	—	—	68	122
(VS2)	2	—	85	9	6	54	—
$TiO_2/V_2O_5/SiO_2$	1	—	100	—	—	53	117
(VS3)	2	100	—	—	—	64	
$TiO_2/V_2O_5/SiO_2$	1	—	100	—	—	113	184
(VS4)	2	100	—	—	—	71	—
$TiO_2 + V/SiO_2$ (VS5)	1	—	97	3	—	193	193

oxygen content increases to a higher value to form the mixed $V_2O_3 + VO$ layer (with the oxygen content of 40–50%). Increasing further the deposition time, the oxygen reduction leads to a formation of layer with a complex mixture of V_2O_5, V_2O_7 and V_5O_9 until the stable V_2O_5 (with the oxygen content of 28.6%) is reached and formed on the film surface. In all cases, from the estimated value of metal (M) and oxygen (O) content by SIMNRA, the type of oxides consisting in the layer can be easily defined. For instance, the M and O content in M_2O_5 is respectively 28.6% and 71.4%, while it amounts to, respectively, 33.3% and 66.7% for MO_2. The SIMNRA fit for RBS spectrum is simulated for (Nt) product, i.e. the areal density (the number of target atoms per unit area). The values of layer-thickness in (nm) are converted from the simulated (Nt) values (in 10^{15} atoms cm^{-2}) using the conversion coefficient and estimated percentage (%) of each oxide presented in the layers. For instance, for the stoichiometric V_2O_5 layer (1) in the sample VS2

$$d\,[\mathrm{nm}] = n\ Nt\ \left[10^{15}\ \mathrm{at\ cm^{-2}}\right],$$

while for layer (2) in the sample, VS2 consisted of 85% TiO_2, 9% VO_2 and 6% SiO_2

$$d\,[\mathrm{nm}] = (0.85m + 0.09n + 0.06p)\ Nt\left[10^{15}\ \mathrm{at\ cm^{-2}}\right],$$

where m, n, p are the corresponding conversion coefficients estimated using the bulk density of different oxides (e.g. ρ (TiO_2) = 4.23 g cm^{-3}, ρ (VO_2) = 4.57 g cm^{-3}, ρ (V_2O_5) = 3.36 g cm^{-3}). In most cases, the thickness could be estimated with a good accuracy, since the layer either consists of only stoichiometric oxide (such as TiO_2, V_2O_5, VO_2) or the mixture of oxides of the same type (such as ($TiO_2 + VO_2$) or ($VO_2 + SiO_2$) mixture). For such a mixture, since the oxygen content is the same (66.7%), the percentage of different oxides can be easily estimated based on the ratio

Table 2. Effect of hydrogenation on selected films: $V_2O_5/TiO_2/SiO_2$ (VS2), $TiO_2/V_2O_5/SiO_2$ (VS4). They were charged by hydrogen twice (denoted, respectively, by H(1) and (H(2)), each charging was at pressure of 1 bar, at temperature of 300 °C and for 3 h. The layer-thickness of each layer (d (nm)), the percentage (%) of each type of oxides (TiO_2, V_2O_5, VO_2) presented in the film were estimated using SIMNRA and the mass density of the bulk (see text). Layer (1) denotes the surface layer. Due to enhanced Si diffusion from the SiO_2 substrate into the film, the mixed TiO_2–VO_2–SiO_2 layer was formed at the film–substrate interface in all cases. The increased thickness of the film (%) due to hydrogenation was estimated for the total film thickness (D (nm)) with respect to that of as-deposited film.

$V_2O_5/TiO_2/SiO_2$ (VS2)	Layer	V_2O_5 (%)	TiO_2 (%)	VO_2 (%)	SiO_2 (%)	d (nm)	D (nm)	Increased thickness
as-deposited	1	100	—	—	—	68	122	—
—	2	—	85	9	6	54	—	—
hydrogenation-1	1	100	—	—	—	62	131	7%
H (1)	2		62.5	26.5	11	56	—	—
—	3		19	19	62	13	—	—
hydrogenation-2	1	100	—	—	—	62	140	15%
H (2)	2	—	48	36	16	37	—	—
—	3	—	7	18	75	41	—	—
$TiO_2/V_2O_5/SiO_2$ (VS4)	Layer	V_2O_5 (%)	TiO_2 (%)	VO_2 (%)	SiO_2 (%)	d (nm)	D (nm)	increased thickness
as-deposited	1	—	100	—	—	113	184	—
—	2	100	—	—	—	71	—	—
hydrogenation-1	1	—	100	—	—	112	184	0%
H (1)	2	100	—	—	—	58	—	—
—	3	—	—	15	85	14	—	—
hydrogenation-2	1	—	100	—	—	111	187	2%
H (2)	2		—	94	6	47	—	—
—	3	—	—	15	85	29	—	—

between different M components, e.g. $t(\%)\ TiO_2 = u(\%)Ti/33.3(\%)$ where $u(\%)$Ti is the estimated percentage of Ti in the layer and 33.3% amounts to the summation of percentage of all metal contents in the layer ($u(\%)Ti + v(\%)V + w(\%)Si = 33.3(\%)$). Some difficulty arises in the thickness conversion for the layer consisting of a mixture of different oxides, such as layer (2) of sample VS1 (V_2O_{5-x}). In this case, it is more difficult to estimate the exact ratio of different oxides based on only the ratio of M contents, since the O content is different for each oxide. We notice here that besides uncertainty in thickness conversion, the ambiguity in determination of the layer thickness is also related to the layer quality itself. Namely, the sputter deposited films may have some porosities or defects and thus the mass density of the film is certainly different from that of the bulk.

The RBS spectrum of $V_2O_5/TiO_2/SiO_2$ film (VS2) is characterized by a large V-peak at an energy around 1250 keV and a large Ti-peak at an energy around 1200 keV from the film, a steep Si- and O edge from the substrate (at a lower energy than that for the VS1 film, since the film thickness is larger). The thickness of the V_2O_5 and TiO_2 layer are quite similar and so are the V- and Ti-content in the film, thus a clear minimum between the V- and T-peak was observed. The TiO_2 was first deposited on the SiO_2 substrate and then the V_2O_5 layer followed in this case. No stoichiometric TiO_2 was found. Instead, a mixed layer ($TiO_2 + VO_2 + SiO_2$) with a thickness of 54 was formed (layer 2, sample VS2) as a consequence from some Si diffusion (6% SiO_2) and V-diffusion (9% VO_2) into the TiO_2 film. However, the surface layer with a thickness of 68 nm consists of only stoichiometric V_2O_5.

In the case of two $TiO_2/V_2O_5/SiO_2$ films (VS3 and VS4), i.e. deposition sequence is first the vanadium and then the titanium oxide, our analysis reveals that each film consists of only stoichiometric V_2O_5 and TiO_2 layer. For the VS3 film, the thickness of TiO_2 (64 nm) and V_2O_5 layer (53 nm) is in the same order of magnitude. Besides, the film is quite thin. Thus, the V- and Ti- signal was combined into one large peak at around 1200 keV in the RBS spectrum. For the VS4 film, the thickness of TiO_2 layer is estimated to be 113 nm, while it equals 71 nm for V_2O_5 layer (see table 2). Both layers are thicker than those of VS3. Besides, the thickness of TiO_2 film is about 1.5 times larger than that of the V_2O_5 one, i.e. the Ti content in the film is much larger. This leads to the wide shoulder (V-signal) and the large peak (Ti signal) in the RBS spectra. In the case of TiO_2+V/SiO_2 film (VS5), the V content is estimated to be 1% for the entire film, i.e. the film composition is 97% TiO_2 + 3% VO_2. Since the film is thick (193 nm) and the V-content is small, only a broad peak was observed in the RBS spectrum.

Estimated layer composition and thickness of VO_x–TiO_2 films after each charging with hydrogen are given in table 2. We focus on analyzing the hydrogen charging results on sample VS2 (with V_2O_5 as the surface layer) and VS4 (with TiO_2 as the surface layer). These films were charged by hydrogen twice denoted as H(1) and H(2). The increased thickness of the film (%) due to hydrogenation was estimated for the total film thickness (D (nm)) with respect to that of as-deposited film (=(D(after)-D (before))/D (before charging)). As an example, a comparison of the measured and simulated RBS spectra for the $V_2O_5/TiO_2/SiO_2$ film (VS2) before and after hydrogen charging are shown in figure 3. The Ti-peak

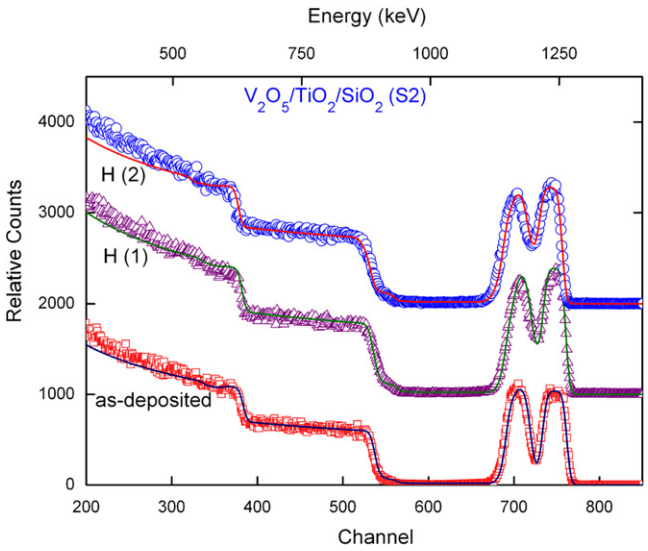

Figure 3. Random RBS (markers) and SIMNRA (lines) simulated spectra for $V_2O_5/TiO_2/SiO_2$ (VS2) before (as-deposited) and after two times of hydrogen charging (denoted, respectively, as H(1) and H(2)). RBS experiments were performed with the incident He^+ ion energy of 1.7 MeV and the backscattering angle of 171°. The curves were normalized and shifted for clarity. The hydrogen charging was seen by e.g. the relative change in the peak-intensity of Ti- and V-signal.

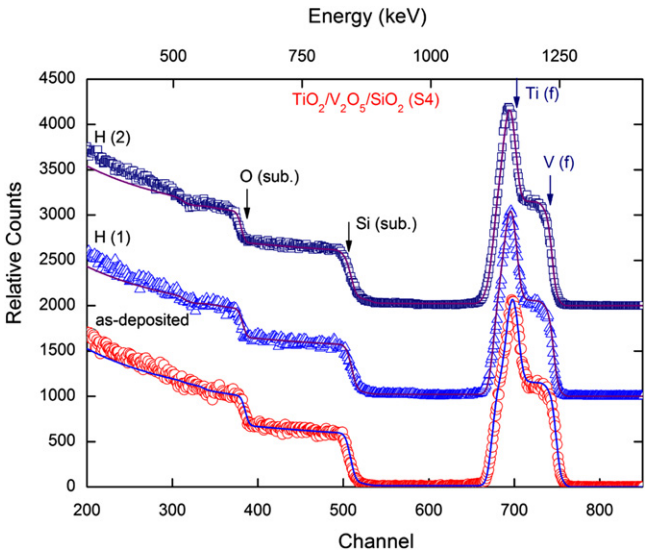

Figure 4. Random RBS (markers) and SIMNRA (lines) simulated spectra for $TiO_2/V_2O_5/SiO_2$ (VS4) before (as-deposited) and after two times of hydrogen charging (denoted respectively as H (1) and H (2)). RBS experiments were performed with the incident He^+ ion energy of 1.7 MeV and the backscattering angle of 171°. The curves were normalized and shifted for a clarity. No visible effect from hydrogen charging was seen.

and V-peak with almost equal intensity before hydrogen charging was observed. The effect of hydrogen charging on this film is revealed by a lowering of the Ti-peak and a widening of this peak at the left hand side. It is caused by a decrease of the percentage of TiO_2 in layer 2 as well as the appearance of an extra mixed layer in the interface (see table 2). The total film thickness is increased, respectively, by 7% and 15% after the first and second hydrogen charging. The thickness change is large enough in this case, which can be seen in the RBS spectrum. No visible hydrogen effect can be seen in RBS spectra from hydrogen charging for the other samples (VS1, VS3, VS4 and VS5). A comparison of the measured and simulated RBS spectra for sample VS4 before and after hydrogen charging is shown in figure 4. The RBS spectra before and after hydrogen charging are similar. The effect from hydrogen charging is mostly revealed by the change of the layer content and layer thickness, but the change in the total thickness is in the range of e.g. 2–3% for VS3 and VS4 film.

We concentrate on analyzing the most visible effect from hydrogen charging, i.e. on the $V_2O_5/TiO_2/SiO_2$ film (VS2). The hydrogen charging leads to a decrease of the layer thickness of the stoichiometric V_2O_5 layer (layer 1) from 68 nm to 62 nm, while that of the mixed $TiO_2 + VO_2 + SiO_2$ layer (layer 2) increases from 54 nm to 56 nm after the first charging. The TiO_2 percentage in layer 2 is only 62.5%, much lower than that before charging (85%). The VO_2 percentage increases from 9% to 26.5%. Besides, an extra layer with the same mixture as that of the layer 2 but with a lower percentage of TiO_2 (19%) and VO_2 (19%) and a higher percentage of SiO_2 (62%) does appear (with a thickness of 13 nm). It can be explained as an enhancement of both Ti diffusion into the SiO_2 substrate and Si diffusion out from substrate into the film. We notice here that the film is heated up to 300 °C for 3 h upon hydrogen charging. It certainly promotes such diffusion and as a consequence increases the thickness of the interface layers. Indeed the second hydrogen charging induces a larger enhancement; the percentage of SiO_2 in the interface layers is largely enhanced and reached even 75%. Our results clearly show the transition from V_2O_5 to VO_2, or in other words, a reduction of V_2O_5 and increase of VO_2 due to hydrogen charging.

We did not construct the depth profile from the RBS data, i.e. the concentration of each element as a function of the film thickness, just because the relative change between different layers is very small. For a clear demonstration of the hydrogen effect, we construct the film diagram, where the layer thickness of different layers is drawn proportionally with respect to the values given in table 2. Different compositions of different oxides in the layers are presented by using different colours. The film diagram was shown for VS2, VS3 and VS4, respectively, in figures 5 and 6, since the hydrogen charging leads to a change of layer thickness (up to 15%) and composition in these cases by hydrogen.

The obtained results on VO_x–TiO_2 films revealed that:

(1) Stoichiometric V_2O_5 and TiO_2 layers were obtained if the deposition sequence was first the vanadium and then the titanium oxide,
(2) The V_2O_5 reduction upon hydrogen charging, i.e. the V_2O_5–VO_2 transition, was always observed,
(3) In the case when the V_2O_5 layer is on the surface, the hydrogen charging effect is much enhanced, indicated by a large increase of the total film thickness (up to 15%

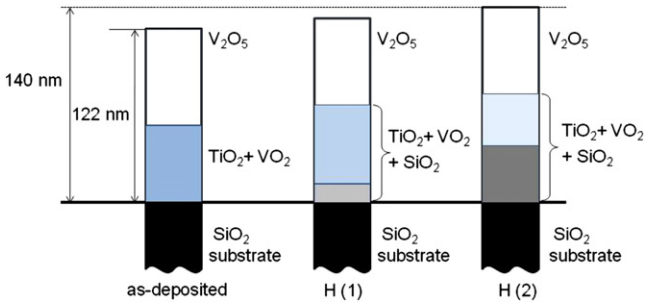

Figure 5. Illustration of the influence of hydrogenation on the structure and composition of $V_2O_5/TiO_2/SiO_2$ film (VS2). The layer thicknesses are drawn proportionally with respect to the values given in table 2. The solid line indicates the original separation between the film and the SiO_2 substrate. Different colours indicate different compositions of different oxides (TiO_2, VO_2, SiO_2) in the layers. The dashed line reveals the film thickness after two times of hydrogenation with respect to that of the as-deposited film (thin solid line). The estimated total film thickness before and after hydrogenation is also given.

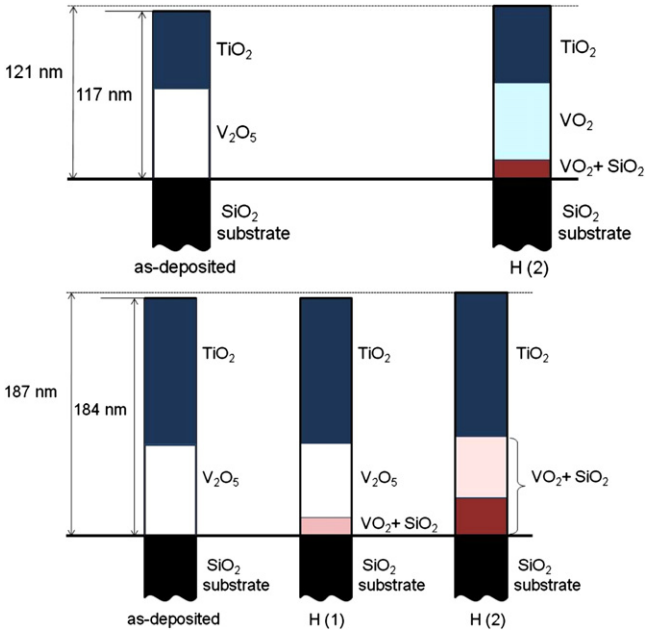

Figure 6. Illustration of the influence of hydrogenation effect on the structure and composition of two films with a similar layer geometry $TiO_2/V_2O_5/SiO_2$ but with a different thickness (VS3 (top), VS4 (bottom)). The layer thicknesses are drawn proportionally with respect to the values given in table 2. The solid line indicates the original separation between the film and the SiO_2 substrate. Different colours indicate different compositions of different oxides (VO_2, SiO_2) in the layers. The dashed line reveals the film thickness after two times of hydrogenation with respect to that of the as-deposited film (thin solid line). The estimated total film thickness before and after hydrogenation is also given.

of its original value after hydrogen charging of 6 h). It reveals the large hydrogen storage in the film,

(4) The V_2O_5 can be well preserved upon hydrogen charging if it locates on the film surface, as in the case of $V_2O_5/TiO_2/SiO_2$ film,

(5) In the case when the TiO_2 layer is on the surface, the film thickness does not change much (only 2–3%) upon hydrogen charging. However, a larger reduction of V_2O_5 is observed. Namely, after 6 h charging, a complete transition of V_2O_5 into VO_2 can be obtained. It indicates that the TiO_2 layer acts as 'hydrogen catalyst' for such V_2O_5–VO_2 transition.

(6) The results obtained for $TiO_2 + V/SiO_2$ film confirmed that no hydrogen is accumulated in TiO_2 even if it is doped with vanadium. However, in this case, since the V-doping is very small (1%) and the film is thick, VO_2 (3%) exists in the film. Thus there is no possibility to observe the V_2O_5–VO_2 transition.

4. Concluding remarks

The most important finding of our investigations is that hydrogen can be stored largely in the Ti layer (with hydrogen content to 50%) in thin films of Ti–TiO_2 system and that palladium could act as a good catalyst for hydrogen diffusion into the films. A large hydrogen absorption can be obtained in the thin films of VO_x–TiO_2 system if the surface layer is the V_2O_5 layer. Besides, the introduction of hydrogen could also remove the Ti preferential orientation and/or induce a V_2O_5–VO_2 transition in the films.

Acknowledgments

The authors highly acknowledged the great help and fruitful cooperation of A Brudnik (AGH Krakow), S Flege and C Schmitt (Damstadt University of Technology), D Rogalla and H-W Becker (Dynamitron Tandem Lab, Ruhr-Universität Bochum), R Kužel and V Sechovsky (Charles University). We acknowledge the support of the Czech-Polish cooperation by the Czech Ministry of Education (Czech-polish project 7AMB14PL036 (9004/R14/R15). N-THKN acknowledged the financial support by the European Regional Development Fund under the Infrastructure and Environment Programme.

References

[1] Yan Q, Lei Y, Yuan J and Coat J 2010 *Technol. Res.* **7** 229
[2] Jacobson P, Li S-C, Wang C and Diebold U 2008 *J. Vac. Sci. Technol.* B **26** 2236
[3] Ankerhold G, Mitsehke F, Frerking D, Ristau D, Mlynek J and Lange W 1989 *Appl. Phys.* B **48** 101
[4] Fujishima A and Honda K 1972 *Nature* **238** 37
[5] Linsebigler A L, Lu G and Yates J T Jr 1995 *Chem. Rev.* **95** 735
[6] O'Regan B and Grätzel M 1991 *Nature* **353** 737
[7] Varghese O K and Grimes C A J 2003 *Nanosci. Nanotech.* **3** 277
[8] Fujishima A, Zhang X and Tryk D A 2008 *Surf. Sci. Rep.* **63** 515
[9] Henderson M A 2011 *Surf. Sci. Rep.* **66** 185
[10] Baraton M-I 2011 *Open Nanosci. J.* **5** 64
[11] Pillai P, Raja K S and Misra M 2006 *J. Power Sources* **161** 524
[12] Choi B J *et al* 2005 *J. Appl. Phys.* **98** 033715
[13] Kim W-G and Rhee S-W 2010 *Microelectron. Eng.* **87** 98

[14] Ohkoshi S, Tsunobuchi Y, Matsuda T, Hashimoto K, Namai A, Hakoe F and Tokoro H 2010 *Nat. Chem.* **2** 539
[15] Rosaiah P and Hussain O M 2013 *Advanced Nanomaterials and Nanotechnology (Springer Proceedings in Physics)* vol 143 (Berlin: Springer) p 485
[16] Zhang L T, Song J, Dong Q F and Wu S T 2009 *Adv. Mater. Res.* **79–82** 931
[17] Zhang Q *et al* 2001 *J. Mater. Sci. Technol.* **17** 417
[18] Honicke D and Xu J 1988 *J. Phys. Chem.* **92** 4699
[19] Xie Y C and Tang Y Q 1990 *Adv. Catal.* **37** 1
[20] see e.g. Centi G 1996 *Appl. Catal.* A **147** 267
[21] Mlyuka N R, Niklasson G A and Granqvist C G 2009 *Sol. Energy Mater. Sol. Cells* **93** 1685
[22] Brudnik A, Czternastek H, Zakrzewska K and Jachimowski M 1991 *Thin Solid Films* **199** 45
[23] Kim-Ngan N-T H, Balogh A G, Meyer J D, Brötz J, Hummelt S, Zając M, Ślęzak T and Korecki J 2008 *Surf. Sci.* **602** 2358
[24] Kim-Ngan N-T H, Balogh A G, Meyer J D, Brötz J, Zając M, Ślęzak T and Korecki J 2009 *Surf. Sci.* **603** 1175
[25] Drogowska K, Tarnawski Z, Brudnik A, Kusior E, Sokołowski M, Zakrzewska K, Reszka A, Kim-Ngan N-T H and Balogh A G 2012 *Mater. Res. Bull.* **47** 296
[26] Tarnawski Z *et al* 2013 *Adv. Nat. Sci.: Nanosci. Nanotechnol.* **4** 025004
[27] Drogowska K, Flege S, Schmitt C, Rogalla D, Becker H-W, Kim-Ngan Nhu–T H, Brudnik A, Tarnawski Z, Zakrzewska K and Balogh A G 2012 *Adv. Mater. Sci. Eng.* **2012** art. 269603